Double three-phase Dual Active Bridge converter for high frequency high current applications

Bernardo Cougo, Thierry Meynard, Henri Schneider

▶ **To cite this version:**

Bernardo Cougo, Thierry Meynard, Henri Schneider. Double three-phase Dual Active Bridge converter for high frequency high current applications. IECON 2012 - 38th Annual Conference of IEEE Industrial Electronics, Oct 2012, Montreal, Canada. pp.350-355, 10.1109/IECON.2012.6388621 . hal-03942944

HAL Id: hal-03942944

https://ut3-toulouseinp.hal.science/hal-03942944v1

Submitted on 15 Jan 2025

HAL is a multi-disciplinary open access archive for the deposit and dissemination of scientific research documents, whether they are published or not. The documents may come from teaching and research institutions in France or abroad, or from public or private research centers.

L'archive ouverte pluridisciplinaire **HAL**, est destinée au dépôt et à la diffusion de documents scientifiques de niveau recherche, publiés ou non, émanant des établissements d'enseignement et de recherche français ou étrangers, des laboratoires publics ou privés.

Distributed under a Creative Commons Attribution - NonCommercial 4.0 International License

Double Three-Phase Dual Active Bridge Converter for High Frequency High Current Applications

B. Cougo, T. Meynard
LAPLACE, Université Toulouse
2 rue Charles Camichel
31071 Toulouse, France
Email: cougo@laplace.univ-tlse.fr

H. Schneider
LAAS, CNRS
7 av. du Colonel Roche
31077 Toulouse, France
Email: hschneid@laas.fr

In a world of growing need for efficient energy conversion and distributed generation, Dual Active Bridge (DAB) converters represent a prominent converter topology given its soft switching properties and the low number of components, which allow the converter to be highly compact. Depending on the operating voltages and the transferred power, large circulating currents may occur. Parallel connection of converters is a good option in high current applications in order to adapt the converters to the use of standard semiconductors. Interleaving techniques provide, to both sides of the DAB converter, the reduction of the current ripple and the increase of its frequency. As a consequence the filters associated to the converter may be reduced. This paper introduces a new topology of DAB (named DABD3) which has a double three-phase connection in the low voltage (LV) high current side of the converter. This topology allows Zero Current Switching (ZCS) in the high voltage (HV) side switches. It has the same number of switches with the same blocking voltage of a parallel association of three single phase DAB converters. However, it presents lower ripple in the DC bus current and lower switched current in the LV side, which reduces the losses of the whole system.

I. Introduction

Parallel and/or series operation of converters allows the increase of the converted power while using standard semiconductors. Interleaving the switching signals of commutation cells reduces the current ripple and increases the dynamic performance converters [1][2].

Paralleling techniques can be applied to many different types of power converters, such as: Flyback [3][4], boost [5], AC choppers [6], and especially in regular DC choppers [2] and inverters [7]. In recent years there is a growing need of the parallelization of bidirectional DC-DC converters due, in great part, to the increase of distributed generation [8,9] and automotive power electronics [10]. A promising converter for bidirectional isolated DC-DC applications is the Dual Active Bridge (DAB) converter, which the most typical configuration is shown in Fig. 1. It is used in several applications having different modulation strategies, where the most common allows Zero Voltage Switching (ZVS) [11] and/or Zero Current Switching (ZCS) [12].

In application such as smart grids, it is common to find a great difference between the voltage in the DC bus of the two sides of the converter [9,13]. So, it is a natural solution to connect DAB converters in series in the HV side in order to use high performance switches with lower breakdown voltage. The LV side usually handles high current and so it is all natural to connect DAB converters in parallel. An example of parallel connection in the LV side and series connection in the HV of DAB converters is shown in Fig. 2, where there are 3 interleaved DAB converters (called here S3DAB).

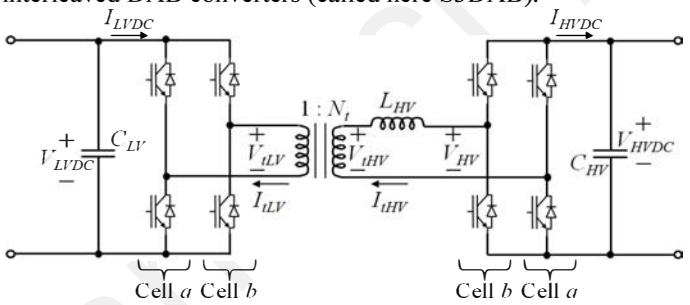

Fig. 1. Typical Dual Active Bridge (DAB) converter.

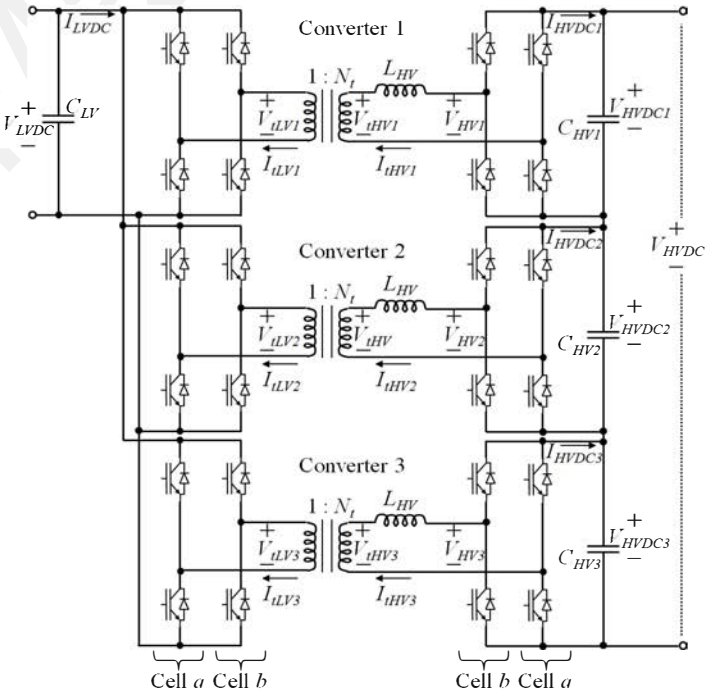

Fig. 2. DAB converter with series connection at HV side and parallel connection at the LV side. This converter is called here S3DAB.

II. Dual Active Bridge Modulation

DAB converters are classically modulated applying a square wave of duty cycle of 50% in each side (V_{tLV} and V_{HV} in Fig. 1) and changing the phase shift (φ) between these two voltages. The resulting current in the transformer has a quasi trapezoidal shape as the one shown in Fig. 3a. This modulation allows Zero

Voltage Switching (ZVS) in all switches in a certain power range [14] and reduced RMS current through the transformer depending on the maximum phase shift allowed in the system. However the switches in the HV side, which usually have a high breakdown voltage, present poor switching performance and consequently a modulation with ZCS at these switches is desired [13].

Triangular modulation allows ZCS at the HV side switches [13, 14] which can be seen by the relevant voltage and current waveforms shown in Fig 3b. In this type of modulation phase shift is zero and, in the case where $V_{LVDC} \cdot N_t > V_{HVDC}$ (where V_{LVDC}, V_{HVDC} and N_t are respectively the DC voltages at the LV and HV sides and the turns ratio of the transformer), duty cycles in the HV and LV sides, respectively D_{HV} and D_{LV}, can be calculated as:

$$D_{HV} = \frac{\sqrt{(N_t \cdot V_{LVDC} - V_{HVDC}) \cdot N_t \cdot L_{HV} \cdot V_{LVDC} \cdot P_t \cdot T_s}}{(N_t \cdot V_{LVDC} - V_{HVDC}) \cdot V_{LVDC} \cdot T_s} \quad (1)$$

$$D_{LV} = \frac{V_{HVDC} \cdot D_{HV}}{N_t \cdot V_{LVDC}} \quad (2)$$

where L_{HV} is the inductance in the HV side of the transformer, P_t is the transferred power and T_s is the switching period.

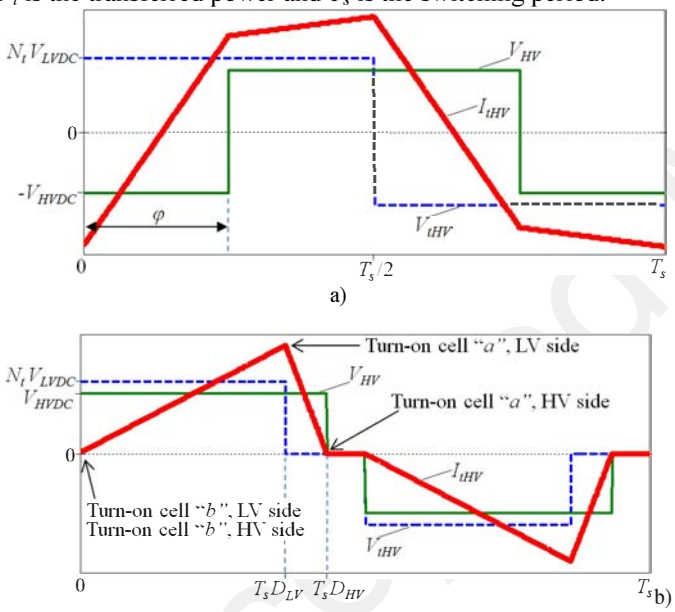

Fig. 3. Relevant voltages and currents of a DAB converter using a) phase shift modulation and b) triangular modulation.

Note that this modulation, although achieving ZCS at the HV side switches, imposes the LV side switches to commutate at the maximum value of the current of the switching period. This may induce high switching losses at the LV side semiconductors. This can be reduced if using the proposed three-phase topology (DABD3) of this paper, which will be explained in Section III.

A. DC bus current

For the DAB converter of Fig. 1, the current flowing in the DC bus of the LV side (I_{LVDC}) of the converter is equal to the current on the LV side of the transformer (I_{tLV}), but switched by LV full bridge. The resulting waveform is shown in Fig. 4a. In the same manner, the current flowing in the DC bus of the HV side (I_{HVDC}) of the converter is equal to the current on the HV side of the transformer (I_{tHV}), but switched by HV full bridge. The resulting waveform is also shown in Fig. 4a. Neglecting the magnetizing current of the transformer, $I_{tLV} = I_{tHV} \cdot N_t$.

Both currents of Fig. 4a have high ripple compared to the DC value. This may induce high losses on the conductors connected to DC bus capacitors. It also highly influences the amount of capacitance necessary in each side to maintain a reasonable value of voltage ripple. Thus, in the case of parallel connection of the LV side converters (e.g. Fig 2), the ripple in the DC bus current can be reduced and the apparent frequency of the current ripple is increased. This is shown in Fig 4b, where the DC bus current at the LV side is plotted for a number of paralleled converters (N_p) equal to 1, 2, 3, and 6, operating at the same point, transferring the same total power from the LV side to the HV side. With the current ripple reduction and the apparent frequency increase, capacitor C_{LV} and eventual input filter size can be significantly reduced.

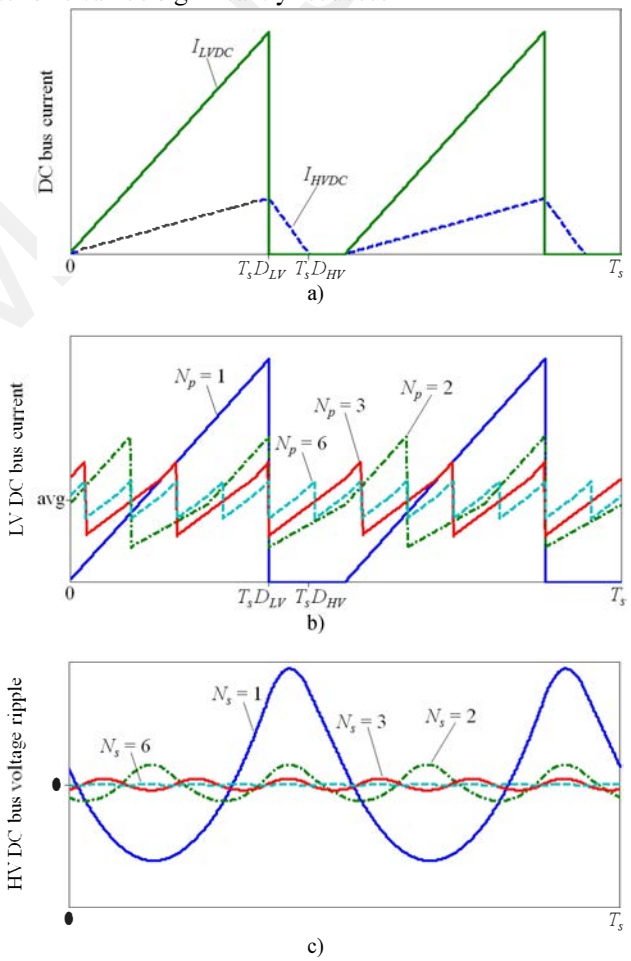

Fig. 4. a) Current in the LV and HV DC buses of a single-phase DAB converter with triangular modulation; b) current in the LV DC bus and c) voltage in the HV DC bus of interleaved DAB converters with parallel connection in the LV side and series connection in the HV side, using triangular modulation.

When converters are connected in series in the HV side, the current flowing through each bus capacitor (C_{HVn} in Fig. 2) is practically equal to current corresponding to its own converter and so the resulting capacitance needed to keep each individual

voltage ripple (V_{HVDCn} in Fig. 2) within a certain limit is not reduced by the interleaved characteristic of the entire converter. However, since the voltage ripple in the HV side of the entire converter (V_{HVDC} in Fig. 2) is equal to the sum of the voltage ripple in each capacitor ($\sum V_{HVDCn}$) and since the individual capacitor voltages have different phase shifts due to interleaved switching signals, V_{HVDC} has a very low ripple. Thus, increasing the number of series connected interleaved converters may reduce the size of eventual filters needed between the bus capacitors and the HV DC source/load.

The reduction in the DC bus voltage ripple and the increase of the apparent frequency are shown in Fig 4c for a number of series connected converters (N_s) equal to 1, 2, 3, and 6, operating at the same point, transferring the same total power from the HV side to the LV side.

Section III will show that the proposed DABD3 reduces the current ripple in the LV side bus capacitor and it also reduces the total voltage ripple in the HV side capacitors.

III. Novel Double Three-Phase DAB Converter (DABD3)

Analysis of this structure will be only present for half a switching period as it is commonly done for DAB converters since waveforms are symmetrical to half cycle point.

The structure of the new double three-phase DAB converter, named DABD3, is shown in Fig. 5. The HV side of the converter is the same as in the three interleaved single phase of Fig. 2. However, the HV side winding of each transformer of Fig. 2 is split in two and wound in two different transformers. Analysis of this new three-phase DAB will be done for these 3 full bridges in series at the HV side, as shown in Fig. 5. However, the operation of the converter and all the analysis presented in this section can be extended to any converter in the HV side which can apply a three-level voltage in the transformers, such as Neutral Point Clamped (NPC) converter, a Flying Capacitor (FC) converter, independently if they are connected in series or in parallel.

The LV side of the DABD3 is also similar to that of three interleaved paralleled full bridges of Fig. 2. Each LV side winding of each transformer of Fig. 2 is also split in two and wound in two different transformers. However, the difference is that the middle point of these two split windings are connected in a common node to the corresponding middle point of split windings of the other two phases, as shown in Fig. 5. This common node, which is represented by point Y in Fig. 5, is a floating point which has the voltage V_{LVY} equal to

$$V_{LVY} = \frac{V_{LV1a} + V_{LV1b} + V_{LV2a} + V_{LV2b} + V_{LV3a} + V_{LV3b}}{6} - \frac{V_{HV1} + V_{HV2} + V_{HV3}}{6} \cdot \frac{1}{N_t} \tag{3}$$

In the LV side of the DABD3, the voltage in each "half" winding is equal to the difference between the voltage applied by each bridge leg (V_{LVmn} where m=1,2,3 and n=a,b) and the voltage in the node Y. Having this information and noting the transformer dots in Fig. 5, the voltage reflected to the HV side of the transformer (V_{tHVm} where m=1,2,3, in Fig. 5) can be calculated. For example, in phase 1, V_{tHV1} is:

$$V_{tHV1} = Nt \cdot \left[\left(V_{LV1a} - V_{LVY}\right) + \left(V_{LV1b} - V_{LVY}\right) \right] = Nt \cdot \left(\frac{2V_{LV1a} + 2V_{LV1b} - V_{LV2a} - V_{LV2b} - V_{LV3a} - V_{LV3b}}{3} \right) + \frac{V_{HV1} + V_{HV2} + V_{HV3}}{3} \tag{4}$$

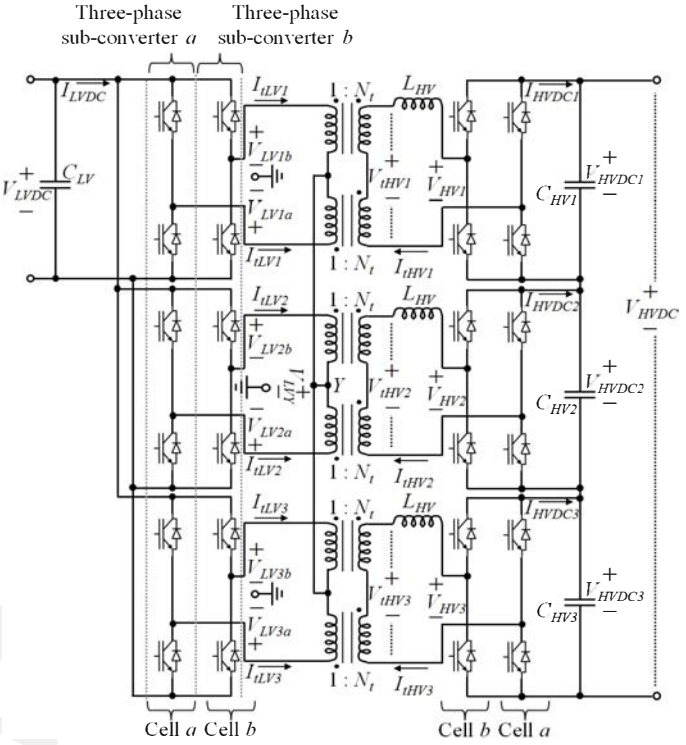

Fig. 5. Double three-phase DAB converter proposed in this paper with series connection at HV side.

This is not a 3-level voltage as in the case of single phase DAB, as it can be seen in Fig. 6, where it is also shown the voltage applied at the HV full bridge (V_{HV1}). The difference between these two voltages is the voltage ($V_{L,HV1}$) applied to the inductor L_{HV}, which can be calculated as in (5). The resulting current waveform in the transformer is also shown in Fig. 6.

$$V_{L,HV1} = Nt \cdot \left(\frac{2V_{LV1a} + 2V_{LV1b} - V_{LV2a} - V_{LV2b} - V_{LV3a} - V_{LV3b}}{3} \right) - \frac{2V_{HV1} - V_{HV2} - V_{HV3}}{3} \tag{5}$$

Rearranging (5) it is clearer the double three-phase nature of the system. This is shown in (6) where one can see that the voltage over the inductor is equal to the sum of voltages of two three-phase systems on the LV side minus the voltage of a three-phase system on the HV side.

$$V_{L,HV1} = Nt \cdot \left(\left(V_{LV1a} - V_{N,LVa}\right) + \left(V_{LV1b} - V_{N,LVb}\right) \right) - \left(V_{HV1} - V_{N,HV}\right) \tag{6}$$

where $V_{N,LVa}$, $V_{N,LVb}$ and $V_{N,HV}$ are virtual neutral voltages to its corresponding three-phase converter

$$V_{N,HV} = \frac{V_{HV1} + V_{HV2} + V_{HV3}}{3}$$
$$V_{N,LVa} = \frac{V_{LV1a} + V_{LV2a} + V_{LV3a}}{3} \tag{7}$$
$$V_{N,LVb} = \frac{V_{LV1b} + V_{LV2b} + V_{LV3b}}{3}$$

Accepted

As it can be seen by (6) and (7) and voltage and current waveforms in Fig. 6, there are many intervals and modes which have to be used to calculate the current, transferred power and duty cycle. To simplify the analysis of all these modes and to approximate this analysis to the one made for the single-phase DAB, we will define virtual voltages in the LV side, $V_{VLVm} = V_{LVma} + V_{LVmb}$, where m=1,2,3. Like this, (6) becomes

$$V_{L,HV1} = Nt \cdot \left(V_{VLV1} - V_{N,VLV}\right) - \left(V_{HV1} - V_{N,HV}\right) \tag{8}$$

To analyze the system, the different modes must be identified. Each mode consists on a specific sequence of switching instants of each of the phases. If we define, as in the triangular modulation of a single-phase DAB, that phase-shift is equal to zero, $V_{LV} \cdot N_t > V_{HV}$ and $D_{HV} > D_{LV}$, all possible modes can be reduced to only 9, which are shown in Table I.

Table I. Different operation modes for the DABD3, considering that $D_{HV} > D_{LV}$, $V_{LV} \cdot N_t > V_{HV}$ and φ=0. Only modes 1, 2, 6, 7 and 9 are suitable to be used.

Mode Number	D_{LV} (LV side)		D_{HV} (HV side)	
	D_{LVmin}	D_{LVmax}	D_{HVmin}	D_{HVmax}
1	0	1/6	D_{LV}	1/6
2	0	1/6	1/6	D_{LV}+1/6
3	0	1/6	D_{LV}+1/6	1/3
4	0	1/6	1/3	D_{LV}+1/3
5	0	1/6	D_{LV}+1/3	1/2
6	1/6	1/3	D_{LV}	1/3
7	1/6	1/3	1/3	D_{LV}+1/6
8	1/6	1/3	D_{LV}+1/6	1/2
9	1/3	1/2	D_{LV}	1/2

Further analysis, which will not be shown here for the purpose of conciseness, show that only modes 1, 2, 6, 7 and 9 can be used to efficiently transfer power from one side of the converter to the other.

For each mode, the voltage over the inductor must be calculated and for each interval the inductor current must be calculated in order to find the values of D_{LV} and D_{HV} which imposes a ZCS at the HV side switches, for a given transferred power P_t and inductor L_{HV}. An example of the intervals used to calculate the inductor current, for mode 9, is given in Fig. 7.

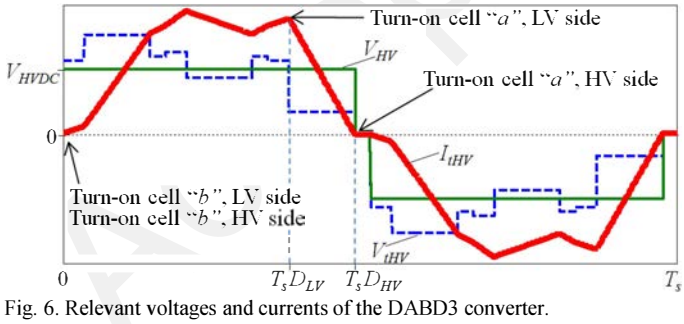

Fig. 6. Relevant voltages and currents of the DABD3 converter.

For this mode, if only interval I is taken as an example to show the value of the voltage applied to the inductor, we note that [using (5)]:

$$V_{L,HV1} = Nt \cdot V_{LVDC}\left(\frac{2(1)-(1)-(-1)}{3}\right) - V_{HVDC}\left(\frac{2(1)-(1)-(-1)}{3}\right) = \frac{2}{3}\left(Nt \cdot V_{LVDC} - V_{HVDC}\right) \tag{9}$$

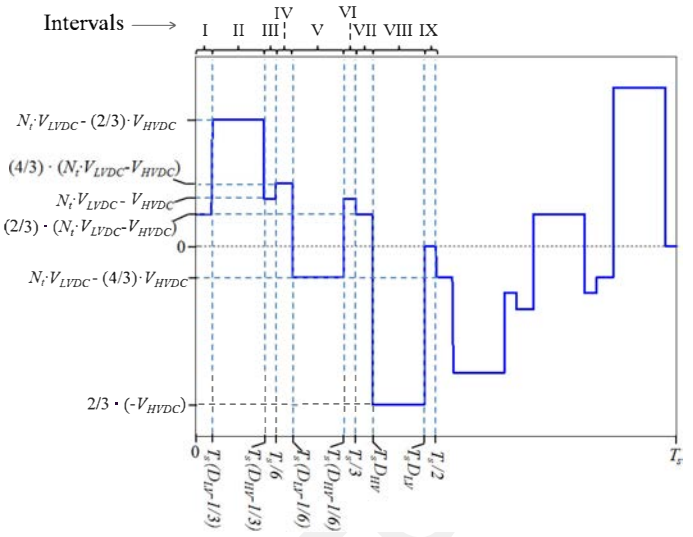

Fig. 7. Inductor voltage ($V_{L,HV1}$) showing all the intervals used to calculate the inductor current, with corresponding voltage value and instants where intervals are changed. Example given for mode 9.

This approach can be used to all intervals and consequently the voltage applied to the inductor in each interval can be calculated (as in the example of mode 9 shown in Fig. 7).

For each mode, one can solve a set of equations and, independently of the transferred power P_t and inductor L_{HV}, find the relationship between D_{LV} and D_{HV} which impose the switches at HV side to switch at zero current. Formulas to calculate the transferred power for the case of ZCS at HV side switches, for a given L_{HV}, will not be shown here for a matter of space. However, the formula for mode 9 is given below since it will be used in the next section in the comparison of the DABD3 with the 3 interleaved single phase DABs.

$$P_t = \frac{N_t \cdot V_{LVDC} \cdot \left(N_t \cdot V_{LVDC} - V_{HVDC}\right) \cdot \left(1 + 6 \cdot D_{LV}\right)^2}{18 \cdot f_s \cdot L_{HV}} \tag{10}$$

For modes 2, 6 and 7, there is no solution for ZCS in both half bridge legs. So Table III shows the formulas for modes 2, 6 and 7 which impose ZCS in the three-phase sub-converter "a" (the one which impresses voltages V_{LV1a}, V_{LV2a} and V_{LV3a}).

IV. Comparison between DABD3 and 3 Interleaved Single Phase DABs

Smart grid applications are chosen to illustrate the advantages of the DABD3 (Fig. 5) over 3 interleaved DAB converters connected in parallel in the LV side and in series in the HV side (called here S3DAB). The parameters used in the comparison are given in Table IV. Given the high voltage at the HV side, 1.7kV switches might be used in the HV side. Switches with such breakdown voltages have poor switching performance, and therefore ZCS in these switches is desired.

Given that 3 converters are connected in series in the HV side, the DC bus voltage in each converter is V_{HVDCn} = 1kV. Having 400V in one side and 1kV in the other side, the turns ratio of the transformer which reduces the RMS current in both sides is N_t = 3, which is the minimum integer number higher than 1000V/400V [14].

Table III. Relationship between D_{HV} and D_{LV} for ZCS at the HV side switches and transferred power formulas at this operation. This is shown for modes which suitable to be used in the DABD3.

Mode Number	Relationship between D_{LV} and D_{HV}
1	$D_{HV} = \frac{N_t \cdot V_{LVDC} \cdot D_{LV}}{V_{HVDC}}$
2	$D_{HV} = \frac{V_{HVDC} + 6 \cdot N_t \cdot V_{LVDC} \cdot D_{LV}}{12 \cdot V_{HVDC}}$
6	$D_{HV} = \frac{V_{HVDC} - N_t \cdot V_{LVDC} + 12 \cdot N_t \cdot V_{LVDC} \cdot D_{LV}}{12 \cdot V_{HVDC}}$
7	$D_{HV} = \frac{-V_{HVDC} - N_t \cdot V_{LVDC} + 12 \cdot N_t \cdot V_{LVDC} \cdot D_{LV}}{6 \cdot V_{HVDC}}$
9	$D_{HV} = \frac{-V_{HVDC} + N_t \cdot V_{LVDC} + 6 \cdot N_t \cdot V_{LVDC} \cdot D_{LV}}{6 \cdot V_{HVDC}}$

Table IV. System parameters used to compare DABD3 and S3DAB.

Parameter	Value
HVDC bus voltage ($3 \cdot V_{HVDC}$)	3kV
LVDC bus voltage (V_{LVDC})	400V
Maximum transferred power (P_{tmax})	300kW (100kW/phase)
Switching frequency (f_s)	20kHz
Total HVDC bus capacitance ($C_{HV}/3$)	30µF
LVDC bus capacitor (C_{LV})	270µF

Choosing that the maximum transferred power (P_{tmax}) will be achieved at the maximum duty cycle $D_{HV} = 0.5$, inductance L_{HV} can be calculated using (10) for the DABD3 and using formulas in [13] for the single phase DABs. They result on, respectively, $L_{HV,DAB3D} = 24.7\mu H$ and $L_{HV,S3DAB} = 20.7\ \mu H$.

Although $L_{HV,DAB3D}$ is 19% greater than $L_{HV,S3DAB}$, this difference does not usually affect the size of the magnetic component since the inductance needed to shape the current is, in general, designed as the leakage inductance of the transformer. The size of the transformer is, for most practical cases, only slightly modified when its leakage inductance changes some few percents.

The number of transformers in the DABD3 is the double when compared to the S3DAB. However since each transformer in the DABD3 has half the voltage when compared to the S3DAB, the core cross-section is also the half (for the same number of turns) and so the maximum core losses is about the same in both topologies. However, since the DABD3 have square wave voltages applied by each half bridge, high core losses is also observed at low power transfer point, as is the case of other three-phase DAB or single-phase DAB using phase-shift modulation.

Another difference between these two converters can be seen at Fig. 8, which shows the variation of the duty cycles in both converters at both sides, for different transferred power values. Note the change in the slope of the duty cycles when changing the operation mode. Since the slope of D_{LV} and D_{HV} in the DABD3 are smaller than that of S3DAB for the range of 30kW to 80kW, S3DAB has finer resolution in the transferred power control in this range.

As an example of current waveforms, Fig. 9a shows the currents in the LV side winding of the transformers (I_{tLV}) for both converters, operating at 90% of the maximum transferred power (from the LV to the HV side). The current switched by the LV side switches at the DABD3 converter is 34% smaller than the corresponding current in the S3DAB, which shows that DABD3 has lower switching losses. The same occurs for the whole transferred power range, as it can be seen in Fig. 9b. However, as it was said before, DABD3 with the modulation developed here does not guarantee ZCS in all bridge legs of the HV side switches at the modes 2, 6 and 7, as it can be seen in Fig. 9c. Nevertheless the switched current is not high (maximum of 18% of the peak current in the HV), and consequently the increase of the switching losses in the HV side switches at a certain transferred power range is not high.

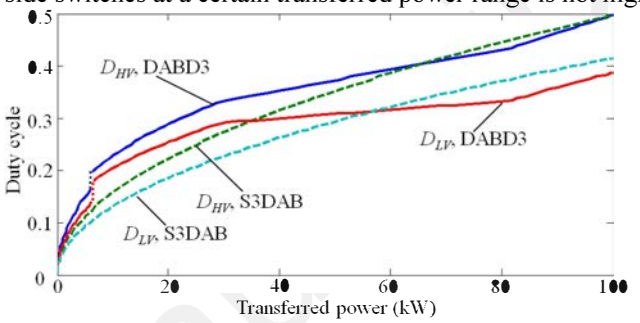

Fig. 8. Duty cycle variation for different transferred power per phase, for DABD3 converter and for 3 interleaved single phase DAB converters.

Not only the peak current is reduced in the DABD3, but also the RMS current which flows in the transformer and in the switches (in a DAB converter, the RMS current value in the transformer is the same as in each of the bridge legs). This is shown in Fig. 9d, where the maximum difference between the RMS values of the currents is equal to 10.5% and the difference at the maximum transferred power is equal to 1.5%. This characteristic of the DABD3 converter shows that it generates lower conduction losses in the switches of both sides of the converter, when compared to the S3DAB converter.

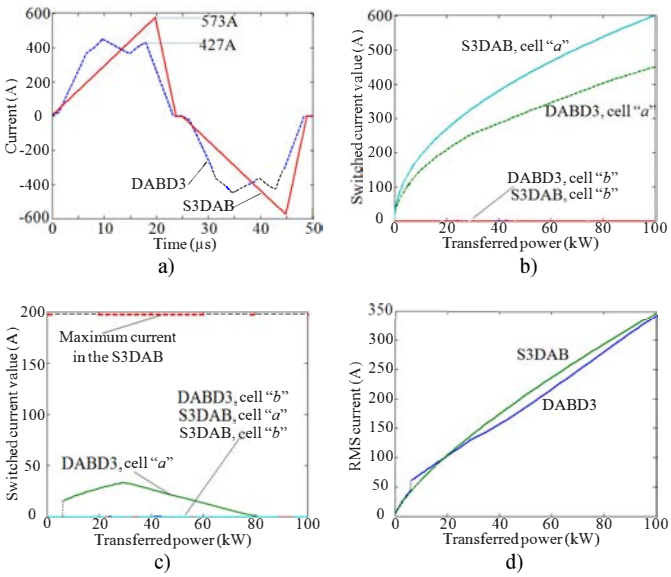

Fig. 9. Comparison of converters DABD3 and S3DAB; a) current waveform in the LV side of the transformer, operating at 90% of the maximum transferred power. Value of the switched current at the bridge legs of the b) LV side converters and c) HV side converters; d) RMS current at each bridge leg of the HV side converters for different transferred power per phase.

Accepted Manuscript

Also the current ripple in the LV DC bus and the voltage ripple in the HV DC bus are reduced in the DABD3. As an example of current waveforms, Fig. 10a shows the currents in the LV DC bus and the HV DC bus voltage (respectively I_{LVDC} and V_{HVDC}, in Fig. 3 and Fig. 5) for both converters, operating at 90% of the maximum transferred power (from the LV to the HV side). The apparent frequency of these currents and voltages is 6 times higher than the switching frequency. The current and voltage ripples in the DABD3 converter are, respectively, 25% and 52% smaller than in the S3DAB, which shows that DABD3 requires smaller input capacitor and/or filters to cope with THD and EMI standards related to the application where the converter will be used. The same occurs for the whole transferred power range, as it can be seen in Fig. 10b.

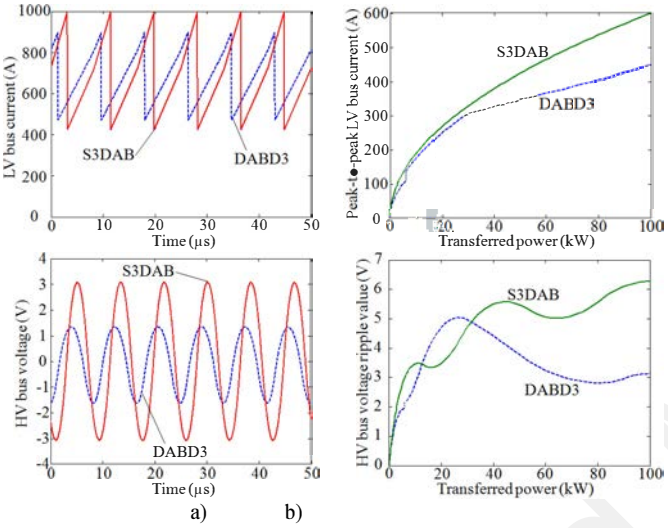

Fig. 10. Comparison of converters DABD3 and S3DAB; a) current waveform in the LV DC bus and voltage waveform of the HV DC bus, with the converters operating at 90% of the maximum power transferred; b) peak-to-peak value of the current ripple in the LV DC bus and the voltage ripple in the HV DC bus for different transferred power per phase.

V. CONCLUSION

This paper presents a new bidirectional isolated DC-DC converter suitable for high frequency and high current applications. The converter, which is named DABD3, has two paralleled three-phase DAB converters at the low voltage side with a common node. The high voltage side converter can be composed by 3 single-phase converter which produces three-level voltages, such as full bridges, NPC or Flying Capacitor converters. In the present paper, though, the analysis was presented with 3 full bridge converters connected in series at the HV side.

Analysis of the different modes used to control the power transfer was presented as well as the modulation methods. Comparison was performed between the new converter and 3 interleaved single phase DAB converters (called here S3DAB), because both converters present the same number of switches having the same switched voltage and carrying about the same RMS current. S3DAB was controlled with triangular current modulation, which reduces switching losses given the ZCS characteristic at the HV side switches.

For the same transferred power, when comparing to the S3DAB, the DABD3 presented lower switched current at the LV side (26% lower at maximum power transfer point) which reduces switching losses in the LV side. Also it presented lower current ripple in the LV DC bus and voltage ripple in the HV DC bus (respectively 25% and 50% lower at maximum power transfer point), which reduces the size of bus capacitors and input filters. In addition it presented slightly lower RMS current in the transformers and in the switches, which reduce transformer and switch losses. However, the new converter does not present ZCS at the HV side for all modes, although switched current at these modes are low. Also, this topology uses the double of the number of transformers, but with, theoretically, approximately half the size of those used in the S3DAB.

VI. REFERENCES

[1] P. Zumel, O. Garcia, J. A. Cobos, and J. Uceda, "Tight magnetic coupling in multiphase interleaved converters based on simple transformers," in *Proc. IEEE Applied Power Electronics Conference*, 2005, pp. 385-391.

[2] P. Wong, Q. Wu, P. Xu, P. Yang, and F. C. Lee, "Performance Improvements of Interleaving VRMs with coupling inductors," *IEEE Trans. Power Electronics*, vol. 16, no. 4, pp. 499-507, 2001.

[3] F. Forest, B. Gelis, J.-J. Huselstein, B. Cougo, E. Laboure, and T. Meynard, "Design of a 28V-to-300V-12kW multi-cell interleaved flyback converter using intercell transformers," *IEEE Trans. Power Electronics*, vol. 25, no. 8, pp. 1966-1974, 2010.

[4] Y.-K. Lo and J.-Y. Lin, "Active-clamping ZVS flyback converter employing two transformers," *IEEE Trans. Power Electronics*, vol. 22, no. 6, pp. 2416-2423, Nov. 2007.

[5] Q. Li and P. Wolfs, "A current fed two-inductor boost converter with an integrated magnetic structure and passive lossless snubbers for photovoltaic module integrated converter applications," *IEEE Trans. Power Electronics*, vol. 22, no. 1, pp. 309-321, Jan. 2007.

[6] C. Haederli, P. Ladoux and T. Meynard, "Variable DC-link voltage source inverter for reactive power compensation in single phase 25kV AC railway systems," *Proc. PCIM*, May 2007.

[7] D. M. Vilathgamuwa, C. J. Gajanayake, and P. C. Loh, "Modulation and control of three-phase paralleled Z-source inverters for distributed generation applications," *IEEE Trans. Energy Conversion*, vol. 24. no. 1, pp. 173-183, 2009.

[8] Tripathi, A.K.; Hatua, K.; Mirzaee, H.; Bhattacharya, S.; , "A three-phase three winding topology for Dual Active Bridge and its D-Q mode control," *Applied Power Electronics Conference and Exposition (APEC), 2012 Twenty-Seventh Annual IEEE* , vol., no., pp.1368-1372, 5-9 Feb. 2012

[9] R. A. Friedemann, F. Krismer, J. W. Kolar, "Design of a Minimum Weight Dual Active Bridge Converter for an Airborne Wind Turbine System", *Applied Power Electronics Conference and Exposition* (*APEC 2012*), Orlando Florida, USA, Feb. 2012.

[10] F. Krismer, J. W. Kolar, "Accurate Small-Signal Model for an Automotive Bidirectional Dual Active Bridge Converter", Control and Modeling for Power Electronics, 2008 (COMPEL 2008). Aug. 2008.

[11] Zhiyu Shen, R. Burgos, D. Boroyevich, and F. Wang, "Soft-switching capability analysis of a dual active bridge dc-dc converter," *Electric Ship Technologies Symposium* (ESTS 2009), pp.334-339, April 2009.

[12] F. Krismer, J. Biela, and J. W. Kolar, "A Comparative Evaluation of Isolated Bi-directional DC/DC Converters with Wide Input and Output Voltage Range," *IEEE Industry Applications Conference*, Oct. 2005.

[13] G. Ortiz, J. Biela, D. Bortis, J. W. Kolar, "1 megawatt, 20 kHz, isolated, bidirectional 12kV to 12kV DC-DC converter for renewable energy applications," IEEE ECCE Asia, Sapporo, Japan, June 2010.

[14] F. Krismer, "Modeling and Optimization of Bidirectional Dual Active Bridge DC-DC Converter Topologies" Ph.D. dissertation, ETH Zürich, 2011.

Accepted Manuscript